HOSTED BY
ELSEVIER
CrossMark
Available online at www.sciencedirect.com
ScienceDirect
Progress in Natural Science: Materials International 25 (2015) 191–196
Progress in Natural Science Materials International
www.elsevier.com/locate/pnsmi
www.sciencedirect.com

Original Research

Spontaneous and continuous anti-virus disinfection from nonstoichiometric perovskite-type lanthanum manganese oxide

Ding Weng[a,b], Chao Lei[a,c], Ting-Ting Wu[d], Ren Sun[d,*], Meiqing Shen[c,*], Yunfeng Lu[a,*]

[a]Department of Chemical and Biomolecular Engineering, University of California, Los Angeles, CA 90095, United States
[b]Department of Orthopedic Surgery, Brigham and Women's Hospital, Harvard Medical School, MA 02115, United States
[c]Key Laboratory for Green Chemical Technology of State Education Ministry, School of Chemical Engineering and Technology and State Key Laboratory of Engines, Tianjin University, Tianjin 300072, China
[d]Department of Molecular and Medical Pharmacology, University of California, Los Angeles, CA 90095, US

Received 24 March 2015; accepted 2 May 2015
Available online 14 July 2015

Abstract

Viral pathogens have threatened human being's health for a long time, from periodically breakout flu epidemics to recent rising Ebola virus disease. Herein, we report a new application of nonstoichiometric Perovskite-type La_xMnO_3 ($x=1$, 0.95, and 0.9) compounds in spontaneous and continuous disinfection of viruses. Perovskite-type La_xMnO_3 ($x=1$, 0.95, and 0.9) is well-known for their catalytic properties involving oxidization reactions, which are usually utilized as electrodes in fuel cells. By utilizing superb oxidative ability of La_xMnO_3 ($x=1$, 0.95, and 0.9), amino acid residues in viral envelope proteins are oxidized, thus envelope proteins are denatured and infectivity of the virus is neutralized. It is of great importance that this process does not require external energy sources like light or heat. The A/PR/8/34H1N1 influenza A virus (PR8) was employed as the sample virus in our demonstration, and high-throughput disinfections were observed. The efficiency of disinfection was correlated to oxidative ability of La_xMnO_3 ($x=1$, 0.95, and 0.9) by EPR and H_2-TPR results that $La_{0.9}MnO_3$ had the highest oxidative ability and correspondingly gave out the best disinfecting results within three nonstoichiometric compounds. Moreover, denaturation of hemagglutinin and neuraminidase, the two key envelope proteins of influenza A viruses, was demonstrated by HA unit assay with chicken red blood cells and NA fluorescence assay, respectively. This unique disinfecting application of $La_{0.9}MnO_3$ is considered as a great make up to current sterilizing methods especially to photocatalyst based disinfectants and can be widely applied to cut-off spread routes of viruses, either viral aerosol or contaminated fluid, and help in controlling the possibly upcoming epidemics like flus and hemorrhagic fever.

Keywords: Disinfect; Influenza A virus; La_xMnO_3; Nonstoichiometric; Perovskite

1. Introduction

Viral pathogens have resulted in many several diseases to human beings, like flu, ADIS, hepatitis, hemorrhagic fever, etc., which remain as threatens even with today's medical development [1–5]. Taking flu pandemics as the example, its severity has been recorded since the 1918 Spanish pandemic, the most serious flu pandemic in human history [1,6]. Preventing the irregular outbreak and controlling the rapid spreading of flu pandemic have attracted great interest in research community, as a result, antiviral drugs and vaccines are considered as the most effective in vivo solutions [7]. However, continue mutating of viruses has brought huge difficulty for human to get prepared before an outbreak taking place. Thus cutting off the spreading pathways of viruses has become important as the in vitro solution [8–10].

Contacting contaminated surfaces and virus-containing aerosol have been recognized as two essential spreading pathways and several detergents have been inspected on the purpose of disinfecting influenza virus during their transmitting [8,11–14]. However, no matter how efficient they are, it is practically

*Corresponding authors.
E-mail addresses: rsun@mednet.ucla.edu (R. Sun), mqshen@tju.edu.cn (M. Shen), luucla@ucla.edu (Y. Lu).
Peer review under responsibility of Chinese Materials Research Society.

http://dx.doi.org/10.1016/j.pnsc.2015.05.003

impossible to continuously sterilize such public areas with huge flowing population by chemicals or UV lights, no mention that the human manipulation is always necessary to carry out this process.

Massive reports have been published about disinfecting materials and nearly all of them were utilizing photocatalysts to kill microbes, in which bacteria received more research interests than virus did [15–22]. Briefly, reactive free radicals that are generated during light illuminating by photocatalysts, for instance doped TiO_2, AgBr–Ag–Bi_2WO_6 nanojuction and our previous reported $CuInS_4Zn_6$ were utilized as mediators to disinfect microbe sand, visible light were preferred by scientists because of UV band's carcinogenic potential [23–33]. Nevertheless, it is Achilles' heel that performance of all these photocatalysts is limited by illuminating conditions, like light intensity, band distribution, etc. To overcome this inherent drawback of photocatalyst based self-disinfecting surfaces, we are considering an alternative solution that can spontaneously disinfect virus without external energy sources, working continuously and silently without using human workforce.

Herein, we located this problem with the outstanding oxidative property of perovskite-type $LaMnO_3$ [34]. Its disinfecting ability was demonstrated on A/PR/8/34H1N1 influenza A virus as spontaneously, continuously and external energy source freely. It is a great advantage that no special supplies are necessary to make it work, especially illumination or high temperature. Comparing with other oxidative chemicals currently used in disinfection like Cl_2, HClO, $KMnO_4$, etc. [35–39], $LaMnO_3$ is less harsh and superior in stability for long-term operation. To the best of our knowledge, this is the first report about disinfecting ability of perovskite-type compounds without illumination.

The family of $LaMnO_3$ compounds is one of the most interesting members of the perovskite oxides. The research attention to them has been attracted as compound with colossal magneto-resistance [40,41], the cathode material for the solid oxide fuel cells [42], and the oxidation catalyst [43,44] since sixty years ago. It is well known that $LaMnO_3$ exhibits promisingly higher oxidative ability comparing to most other perovskite oxides [34,45]. Structural investigations of $LaMnO_3$ have revealed that Mn^{4+} ions are created in $LaMnO_3$ by the presence of vacancies in La and Mn sites [46–49]. For further improving the oxidative ability of $LaMnO_3$, the partial substitution of La by other elements and nonstoichiometry of La/Mn ratio have been extensively studied to increase the Mn^{4+} ions amount by many researchers [50,51].

As illustrated in Scheme 1, $LaMnO_3$ is proposed to oxidize the amino acid residues of envelope proteins on influenza viruses, hemagglutinin (HA) and neuraminidase (NA), deactivate these proteins and eventually neutralized the virus. Taken H1N1 flu virus as an instance, previous research showed that His, Trp and Tyr were included in HA's activate site while Arg and Tyr were in NA's [52–54], which could be easily oxidized and result in the deactivation of entire proteins. Moreover, the oxidative ability of $LaMnO_3$ compounds was also up-tuned in nonstoichiometric way as La_xMnO_3 (x=1, 0.95, and 0.9) to improve its disinfecting ability.

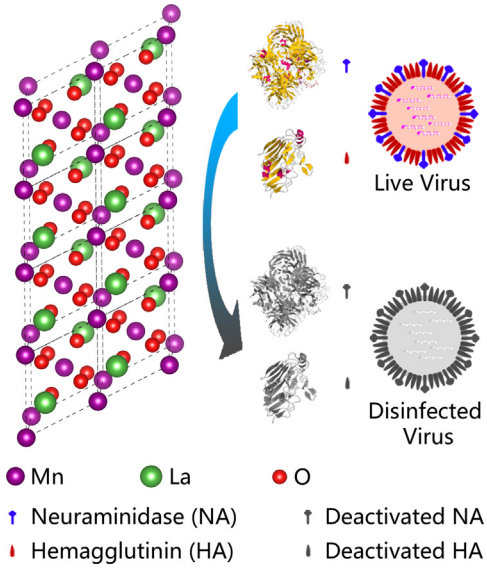

Scheme 1. Oxidization thus disinfection of Influenza A virus by nonstoichiometric perovskite-type La_xMnO_3 (x=1, 0.95, and 0.9)

2. Experimental section

Nonstoichiometric La_xMnO_3 (x=1, 0.95, and 0.9) materials were prepared by the citrate sol–gel method from La$(NO_3)_3 \cdot 6H_2O$ (Aldrich, 99.99%), Mn$(NO_3)_2 \cdot 4H_2O$ (Aldrich, $\geq$ 97.0%) and citric acid (Aldrich, 99.5%). The solutions were prepared in de-ionized water with cation ratio of La:Mn as 1:1, 0.95:1 and 0.9:1, respectively. Then, the citric acid was added with 10 wt% excess over the stoichiometric quantity to insure the complete complexation of metal ions. Hereafter, the solutions were stirred and condensed on a heating stirrer (at 80 °C) until obtaining viscous gels. Then the gels were placed in a vacuum oven (at 90 °C for 12 h) to form spongy raw materials after removing nitrous vapors. Finally the raw materials were crushed and calcined in pure oxygen (at 700 °C for 5 h with a heating rate of 10 °C min^{-1}) and ball-milled (6 min) for further characterization.

The X-ray diffraction (XRD) patterns were obtained with an X'Pert Pro X-ray powder diffractometer equipped with nickel-filtered Cu Kα radiation (λ=1.5418 Å). Data were collected at 45 kV and 40 mA, ranging from 20° to 70° with a 0.02 step size.

Electron paramagnetic resonance (EPR) spectra were recorded at room temperature (RT) with a Bruker A320 spectrometer in the X band frequency (≈ 9.78 GHz). Portions of the samples (20 mg each) were placed inside the quartz probe cell. Locations and the intensity of g factors were determined by Bruker's WINEPR program based on the $h\upsilon = g\beta H$, where h is the Planck constant, H is the applied magnetic field, β is Bohr magneton.

Temperature programmed reduction (TPR) measurements were performed in a conventional, U-shaped, quartz microreactor. The samples (50 mg each) were first heated at 500 °C under a flow of pure O_2 (30 ml min^{-1}) and kept for 30 min. Then, the samples were cooled down to RT in the same pure O_2 flow and followed by purging with helium for 30 min. After that, the samples were heated up at a rate of 10 °C min^{-1}

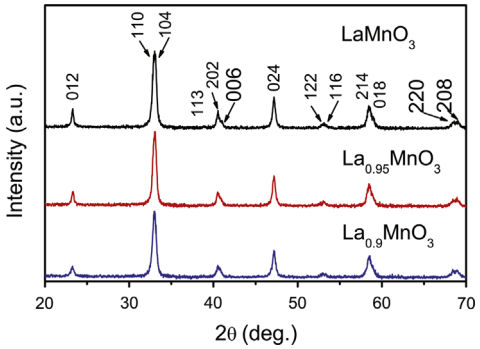

Fig. 1. XRD patterns of the La_xMnO_3 (x=1, 0.95, and 0.9) samples. Peak labels were referred to the publication of Zuo et. al. [52].

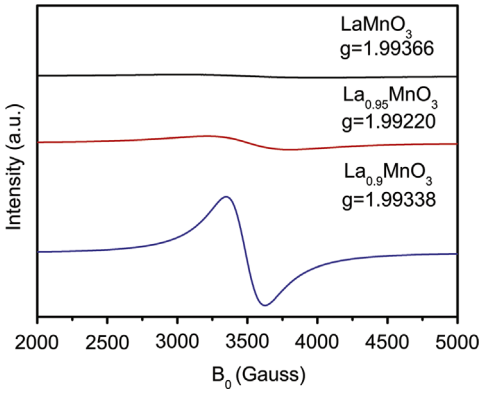

Fig. 2. EPR spectrum of the La_xMnO_3 (x=1, 0.95, and 0.9) samples.

from 50 to 800 °C under a mixed flow containing 5% of H_2 in helium (30 ml min^{-1} as overall flow rate). The concentration of H_2 in the outlet gas was measured by a Balzers QMS200 quadruple spectrometer.

La_xMnO_3 (x=1, 0.95, and 0.9) samples for disinfection experiments were fabricated by drop coating as-prepared materials (40 mg mL^{-1}in aqueous suspension) onto round glass cover slip sand air dried over night at room temperature. The amount of materials was marked by surface concentration, varied from 5 to 20 μg mm^{-2}. The disinfecting ability of as-prepared La_xMnO_3 (x=1, 0.95, and 0.9) samples was examined by $TCID_{50}$ (50% tissue culture infectious dose) assay with A/PR/8/34H1N1 influenza A virus (PR8) on Madin–Darby canine kidney (MDCK) cell line. Cover slips coated with as-prepared La_xMnO_3 (x=1, 0.95, and 0.9) were placed into a 48 well-plate as one slip per well and empty cover slips were set up in the same way as controls. Then PR8 solution (15 μL, 3.57×10^5 $TCID_{50}$ mL^{-1}) was deposit onto each cover slip and the plate was thoroughly wrapped by aluminum foil and placed on ice to prevent PR8 from losing infectivity naturally. Disinfection was carried out for 15 min. Finally PR8 was eluted with sufficient amount of flu growth medium, 10-fold serially diluted and sent to infect the MDCK cells. The infectivity was calculated by the Reed–Muench method after cells were incubated for 72 h with flu growth medium. The experiments were carried out in quadruplicate. Disinfecting efficiency was characterized as relative remaining infectivity.

In hemagglutinin assay, washed pooled chicken red blood cells (10% in Alsever's solution, Lampire Biological Laboratories) were diluted to 1% using PBS buffer solution right before the experiment. After treated by as-coated slips for 2 h (20 μg mm^{-2} of $La_{0.9}MnO_3$), PR8 solution (100 μL at 3.57×10^5 $TCID_{50}$ mL^{-1}) was added into the first column of a Corning V-bottom 96-well plate, which was then 2-fold serially diluted across the 96-well plate with PBS. The final 50 μL of solution from each well in the last column was disposed. Then 50 μL of freshly diluted chicken red blood cells (1%) was added to each well and mixed by gently tapping the plate. The plate was incubated for 30 min at 4 °C and HA Unit (HAU) was observed directly from end point of agglutination phenomena. Experiments were carried out in triplicate.

Neuraminidase assays were carried out in a 48-well plate. As-coated slips (with 20 μg mm^{-2} of $La_{0.9}MnO_3$) were immersed in 30 uL of neuraminidase solution (1UN mL^{-1}, Type V, from Clostridium perfringens) on ice for 1 h. Then 6 μL of solution was taken out and mixed with 50 μL of 2′-(4-Methylumbelliferyl)-α-D-N-acetyl neuraminic acid sodium salt hydrate aqueous solution (5 mM) and 550 μL of sodium acetate buffer (100 mM) with calcium chloride (2 mM). The mixture was incubated at 37 °C for 30 min. Then, 200 μL of glycine buffer (200 mM, pH 10.7) was added and the fluorescence signal from 400 to 500 nm was collected using a Quanta Master Spectrofluorimeter (Photon Technology International) with an exciting wavelength of 365 nm. The emission intensity at 450 nm was used to compare the activity of neuraminidase.

3. Results and discussion

Fig. 1 shows the XRD patterns of La_xMnO_3 (x=1, 0.95, and 0.9) samples calcined at 700 °C. The diffraction patterns of La_xMnO_3 are assigned to a rhombohedral perovskite-structured oxide phase with a space group of $R\bar{3}c$. It is worth noticing that no diffraction peak of Mn_3O_4 phase appeared in the $La_{0.95}MnO_3$ and $La_{0.9}MnO_3$ samples, which is in agreement with other reports [55,56].

The electron configuration of Mn^{4+} ions in an octahedral field ($^4A_{2g}$) allows observing their electron paramagnetic resonance (EPR) spectra at room temperature [57]. Thus, we investigated Mn^{4+} ions signal of the La_xMnO_3 (x=1, 0.95, and 0.9) samples by EPR measurement. As shown in Fig. 2, a unique signal with g-value around 1.99 was detected for all La_xMnO_3 (x=, 0.95, and 0.9) samples, which was correlated with Mn^{4+} ions [58]. Due to the fact that intensity of Mn^{4+} ions is proportion to the double integrated area of EPR spectrum [59], we compared the concentration of Mn^{4+} ions among the La_xMnO_3 (x=1, 0.95, and 0.9) samples. The double integrated area ($La_{0.9}MnO_3 \sim 7.88 \times 10^{11}$; $La_{0.95}MnO_3 \sim 2.95 \times 10^{11}$; $LaMnO_3 \sim 1.14 \times 10^{11}$) increased with decreasing of La/Mn ratio. Therefore, the lower La/Mn ratio achieved the higher concentration of Mn^{4+} ions in the La_xMnO_3 (x=1, 0.95, and 0.9) samples, which correlated to higher oxidative ability [56,60].

The results of H_2-TPR experiments performed on the La_xMnO_3 (x=1, 0.95, and 0.9) samples are depicted in Fig. 3. The La_xMnO_3 (x=1, 0.95, and 0.9) samples were

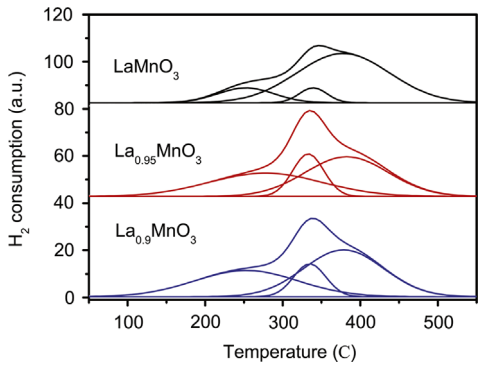

Fig. 3. H_2-TPR profiles of the La_xMnO_3 ($x=1$, 0.95, and 0.9) samples.

Table 1
Integrated peak area of the LaxMnO3 ($x=1$, 0.95, and 0.9) samples

	250–260 °C	330–340 °C	370–380 °C
$LaMnO_3$	155	138	2716
$La_{0.95}MnO_3$	1722	846	2183
$La_{0.9}MnO_3$	2125	993	2829

characterized by the presence of three H_2 reduction peaks based on temperature, which indicated the multiple sites for the reduction of perovskites. The first peak located at the temperature of 250–260 °C was assigned to the removal of non-stoichiometric excess oxygen accommodated within the lattice. The following two peaks located at 330–340 °C and 370–380 °C were attributed to the reduction of Mn^{4+} to Mn^{3+} [60,61]. In order to further investigate the Mn^{4+} ions amount in the La_xMnO_3 (x=1, 0.95, and 0.9) samples, we integrated the peak area and summarized in Table 1. It was noted that the integrated peak area assigned to the reduction of Mn^{4+} to Mn^{3+} in the La_xMnO_3 ($x=1$, 0.95, and 0.9) samples was getting larger while the ratio of La/Mn was decreased, which indicated the more amount of Mn^{4+} ions at $x=0.9$ and corresponded well to the EPR results.

The disinfecting ability of as-prepared La_xMnO_3 ($x=1$, 0.95, and 0.9) samples on PR8 was marked as relative infectivity and summarized in Fig. 4. The experiments were carried out on ice to prevent virus from losing their infectivity naturally. It has been observed that the disinfecting ability was increased with higher surface concentration of La_xMnO_3 and with lower La/Mn ratio (Fig. 4(a)). The best disinfection was achieved by $La_{0.9}MnO_3$ (20 μg mm^{-2}) as 76% of PR8 was neutralized within only 15 min, while no external energy source was supplied, included but not limited to light and heat, also there was no special gas supplies. Specifically 4.0×10^3 $TCID_{50}$ of virus have been disinfected, while the airborne ID_{50} was reported in the range of 0.6–3.0 $TCID_{50}$ [62], which suggested high-throughput disinfection and outstanding handling ability of $La_{0.9}MnO_3$ coatings. Also infectivity of PR8 has been reduced significantly over time as shown in Fig. 4(b). When viruses were eluted right after contacting with 5 μg mm^{-2} of $La_{0.9}MnO_3$, i.e. $T=0$ min, the infectivity of PR8 was not affected, which testified that the reduced infectivity was not due to absorption between La_xMnO_3 ($x=1$, 0.95, and 0.9) and PR8 viral particles. Meanwhile disinfecting progress was observed after different contact durations ($T=15$, 30, and 60 min), which suggested that La_xMnO_3 ($x=1$, 0.95, and 0.9) continuously disinfected the virus, and again the disinfection was not attributed to the absorption between them, in which way the loss of infectivity would not keep changing with time.

By correlating observed different disinfecting efficiencies of La_xMnO_3 ($x=1$, 0.95, and 0.9) samples with oxidative ability comparison of different La/Mn ratios, we confidently believe that the disinfection of PR8 involved the oxidative ability of La_xMnO_3 ($x=1$, 0.95, and 0.9). In detail, $La_{0.9}MnO_3$ has best disinfecting ability in all samples with the same concentration, which suggested that $La_{0.9}MnO_3$ particles oxidized more virus than the other two materials. On the other hand, the theoretical calculation, the previous reports and our EPR and H_2-TPR results all suggested the maximum amount of Mn^{4+} ions in $La_{0.9}MnO_3$ among La_xMnO_3 ($x=1$, 0.95, and 0.9) samples, which indicated the highest oxidative ability of $La_{0.9}MnO_3$ [63–65]. Thus the best disinfecting efficiency of $La_{0.9}MnO_3$ was well explained by its highest oxidative ability.

Fig. 4 illustrates the disinfection of influenza A virus. Fig. 4(a) shows that the disinfecting ability of La_xMnO_3 ($x=1$, 0.95, and 0.9) samples was better with the increase of the surface concentration, indicating that $La_{0.9}MnO_3$ had the best disinfecting ability under the condition that 76% of PR8 was disinfected in 15 min with 20 μg mm^{-2} of $La_{0.9}MnO_3$ and the infectivity of PR8 kept decreasing with time, as shown in Fig. 4(b). Mechanism study showed that hemagglutinin (c) and neuraminidase (d) have been deactivated after treated by $La_{0.9}MnO_3$.

To further specify the mechanism behind disinfecting phenomena, deactivation of the two critical envelope proteins on influenza virus, hemagglutinin (HA) and neuraminidase (NA), by as-prepared $La_{0.9}MnO_3$ was separately investigated. HA could bind sialic acid receptor to introduce virus genome into the cell and NA could cleave the sialic acid residues therefore release the newly reproduced viral particles and prevent them for aggregation. Deactivation of HA was examined by testing the binding ability on red blood cells, which was noted as HA unit (HAU). After contacting with 20 μg mm^{-2} of $La_{0.9}MnO_3$ for 2 h, only half of viral HA were working properly (Fig. 4(c)). On the other hand, activity of NA was characterized by fluorescence substrate after contacting with 20 μg mm^{-2} of $La_{0.9}MnO_3$ for 1 h. Similarly to HA, only 60% of NA's original activity got retained (Fig. 4(d)). These results firmly testified our hypothesis. Meanwhile, the possibility that the oxidative species might penetrate viral particles and damage the genetic materials is not ruled-out [66–68], though we do not have facility to quantify mutation of genetic materials for current experiment with PR8. It could be a direction in the future study.

This disinfection mechanism suggests a wide application of $La_{0.9}MnO_4$ coatings because it is based on amino acid residues but not specific proteins, lipid molecules, or gene sequences. Most recently, rapidly rising threat from Ebola virus has widely caught people's attention not only from academy but also publics [5,69–74]. It is well established that VP40 is the most abundant

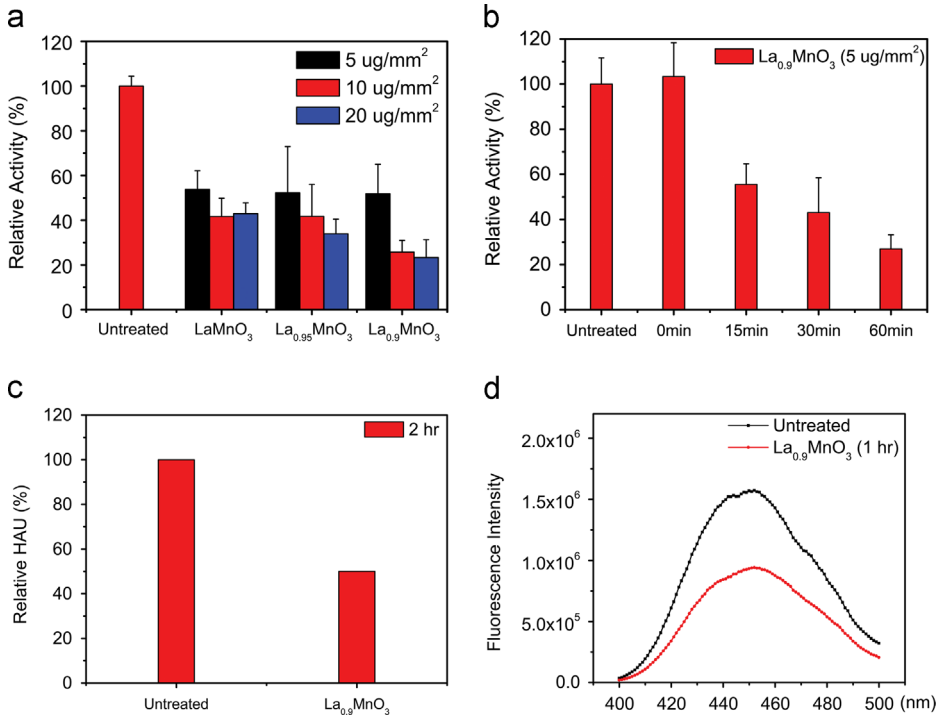

Fig. 4. Disinfection of influenza A virus.

viral structural proteins (~37.7% of viral proteins) that contains conserved amino acid motifs (L-domains) [75–77]. Increasing evidence suggests that VP40 essentially functions as docking sites and facilitates efficient budding through interaction with cellular protein tsg101, a vacuolar protein sorting (vps) pathway in mammalian cells [78–86]. Structural study of VP40 finds out that there are sensitive amino acid residues in conserved amino acid motifs, as Asp, Glu, Gly, Leu, Arg, Thr, Val, and Tyr [31,82,87,88]. These residues are vulnerable to oxidative stress similar to the situation in HA and NA from influenza A virus, thus our $La_{0.9}MnO_4$ coating could be able to denature the VP40 and cutoff the infection of Ebola virus from patient's body fluid. However, lack of accessible Ebola virus to us, this project is waiting for future study.

4. Conclusion

Nonstoichiometric perovskite-type La_xMnO_3 ($x=1$, 0.95, and 0.9) has been successfully synthesized and demonstrated its disinfection of the influenza A virus. This process is spontaneous, continuous and external energy source free. The oxidative ability of La_xMnO_3 ($x=1$, 0.95, and 0.9) is tuned in different stoichiometric ratios and investigated by EPR and H_2-TPR, which $La_{0.9}MnO_3$ owned the best oxidative ability and correspondingly presented the best disinfecting efficiency. As a result, 76% PR8 H1N1 influenza virus was disinfected in 15 min on the coatings containing 20 μg mm^{-2} of $La_{0.9}MnO_3$, which suggested a high-throughput disinfection and sufficient handling ability. We believe that further development of coating, molding and in situ synthesis technology can utilize $La_{0.9}MnO_3$'s feature of anti-pathogens in self-disinfecting air filters and water purification devices. Moreover, due to its oxidizing mechanism, $La_{0.9}MnO_3$ is capable to disinfect wide range of pathogens, like adenovirus, hepatitis C virus, human immunodeficiency virus, Ebola virus, bacteria and even fungus, to prevent potential outbreaks of epidemics and provide safer living environment.

References

[1] C.W. Potter, J. Appl. Microbiol. 91 (2001) 572–579.
[2] B.M. Mathers, L. Degenhardt, H. Ali, et al., Lancet 375 (2010) 1014–1028.
[3] M.J. Alter, E.E. Mast., Gastroenterol. Clin. North Am. 23 (1994) 437–455.
[4] D. Lavanchy, J. Clin. Virol. 55 (2012) 296–302.
[5] M.W. Burnett, J. Spec. Oper. Med. 14 (2014) 93–94.
[6] J.K. Taubenberger, A.H. Reid, T.A. Janczewski, et al., Phil, Trans. R. Soc. Lond. B 356 (2001) 1829–1839.
[7] R.J. Webby, Science 302 (2003) 1519–1522.
[8] M.R. Hilleman, Vaccine 20 (2002) 3068–3087.
[9] S. Jain, L. Kamimoto, A.M. Bramley, et al., N. Engl. J. Med. 61 (2009) 115–119.
[10] S.-W. Yoon, R. Webby, R. Webster., Curr. Top Microbiol. Immunol. 385 (2014) 359–375.
[11] R.H. Alford, J.A. Kasel, P.J. Gerone, et al., Proc. Soc. Exp. Biol. Med. 122 (1966) 800–804.
[12] B. Bean, B.M. Moore, B. Sterner, et al., J. Infect. Dis. 146 (1982) 47–51.
[13] R. Tellier, J. R. Soc. Interface 6 (2009) S783–S790.
[14] J.S. Greatorex, R.F. Page, M.D. Curran, et al., PloS One 5 (2010) e8987.
[15] C. Karunakaran, G. Abiramasundari, P. Gomathisankar, et al., J. Colloid Interface Sci. 352 (2010) 68–74.
[16] K. Shang, S.Y. Ai, Q. Ma, et al., Desalination 278 (2011) 173–178.
[17] C. Karunakaran, A. Vijayabalan, G. Manikandan, et al., Catal. Commun. 12 (2011) 826–829.
[18] K. Chockalingam, A. Ganapathy, G. Paramasivan, et al., J. Am. Ceram. Soc. 94 (2011) 2499–2505.
[19] K. Shang, B. Sun, J.C. Sun, et al., N. J. Chem. 37 (2013) 2509–2514.

[20] D. Venieri, A. Fraggedaki, M. Kostadima, et al., Appl. Catal. B-Environ. 154 (2014) 93–101.
[21] T.D. Pham, B.K. Lee, J. Colloid Interface Sci. 428 (2014) 24–31.
[22] H. Younas, I.A. Qazi, I. Hashmi, et al., Environ. Sci. Pollut. Res. 21 (2014) 740–752.
[23] K.S. Yao, D.Y. Wang, C.Y. Chang, et al., Surf. Coat. Technol. 202 (2007) 1329–1332.
[24] Q. Li, R.C. Xie, Y.W. Ll, et al., Environ. Sci. Technol. 41 (2007) 5050–5056.
[25] P.G. Wu, R.C. Xie, J.K. Shang., J. Am. Ceram. Soc. 91 (2008) 2957–2962.
[26] C.X. Sun, Q. Li, S.A. Gao, et al., J. Am. Ceram. Soc. 93 (2010) 3880–3885.
[27] L.S. Zhang, K.H. Wong, H.Y. Yip, et al., Environ. Sci. Technol. 44 (2010) 1392–1398.
[28] C. Karunakaran, G. Abiramasundari, P. Gomathisankar, et al., Mater. Res. Bull. 46 (2011) 1586–1592.
[29] R.G. Nair, J.K. Roy, S.K. Samdarshi, et al., Colloid Surf. B 86 (2011) 7–13.
[30] L.F. Zhu, C. He, Y.L. Huang, et al., Sep. Purif. Technol. 91 (2012) 59–66.
[31] D. Weng, H. Qi, T.-T. Wu, et al., Nanoscale 4 (2012) 2870–2874.
[32] L. Zhang, M.D. Han, O.K. Tan, et al., J. Mater. Chem. B 1 (2013) 564–570.
[33] T.D. Pham, B.K. Lee., Appl. Surf. Sci. 296 (2014) 15–23.
[34] T. Seiyama, Catal. Rev. 34 (1992) 281–300.
[35] O. Kylin, Sven. Lakartidn. 49 (1952) 416–426.
[36] R.L. Cowie, B.C. Escreet, S. Afr. Med. J. 60 (1981) 304.
[37] E.M. Rodriguez, J.L. Acero, L. Spoof, et al., Water Res. 42 (2008) 1744–1752.
[38] C.W. White, J.G. Martin, Proc. Am. Thorac. Soc. 7 (2010) 257–263.
[39] G.L. Squadrito, E.M. Postlethwait, S. Matalon, Am. J. Physiol. Lung Cell. Mol. Physiol. 299 (2010) L289–L300.
[40] R. von Helmolt, J. Wecker, B. Holzapfel, et al., Phys. Rev. Lett. 71 (1993) 2331–2333.
[41] S. Jin, T.H. Tiefel, M. McCormack, et al., Science 264 (1994) 413–415.
[42] N.Q. Minh, J. Am. Ceram. Soc. 76 (1993) 563–588.
[43] R.J.H. Voorhoeve, D.W. Johnson, J.P. Remeika, et al., Science 195 (1977) 827–833.
[44] C.H. Kim, G. Qi, K. Dahlberg, et al., Science 327 (2010) 1624–1627.
[45] J.H. Kuo, H.U. Anderson, D.M. Sparlin, J. Solid State Chem. 83 (1989) 52–60.
[46] A. Arulraj, R. Mahesh, G.N. Subbanna, et al., J. Solid State Chem. 127 (1996) 87–91.
[47] Q. Huang, A. Santoro, J.W. Lynn, et al., Phys. Rev. B 55 (1997) 14987–14999.
[48] G. Dezanneau, A. Sin, H. Roussel, et al., J. Solid State Chem. 173 (2003) 216–226.
[49] C.N. Munnings, S.J. Skinner, G. Amow, et al., Solid State Ion. 176 (2005) 1895–1901.
[50] H. Wang, Z. Zhao, C.-M. Xu, et al., Catal. Lett. 102 (2005) 251–256.
[51] R. Horyń, R. Klimkiewicz, Appl. Catal. A 351 (2008) 184–188.
[52] J. Stevens, A.L. Corper, C.F. Basler, et al., Science 303 (2004) 1866–1870.
[53] R.J. Russell, L.F. Haire, D.J. Stevens, et al., Nature 443 (2006) 45–49.
[54] J. Gong, W. Xu, J. Zhang., Curr. Med. Chem. 14 (2007) 113–122.
[55] J. Rodríguez-Carvajal, M. Hennion, F. Moussa, et al., Phys. Rev. B 57 (1998) R3189–R3192.
[56] Y. Zuo, J. Li, J. Yi, et al., J. Solid State Chem. 181 (2008) 700–704.
[57] L. Malavasi, C. Ritter, M. Cristina Mozzati, et al., J. Solid State Chem. 178 (2005) 2042–2049.
[58] V.A. Ivanshin, J. Deisenhofer, H.A. Krug von Nidda, et al., Phys. Rev. B 61 (2000) 6213–6219.
[59] D.L. Huber, G. Alejandro, A. Caneiro, et al., Phys. Rev. B 60 (1999) 12155–12161.
[60] A. Machocki, T. Ioannides, B. Stasinska, et al., J. Catal. 227 (2004) 282–296.
[61] S. Ponce, M.A. Peña, J.L.G. Fierro, Appl. Catal. B 24 (2000) 193–205.
[62] T.P. Weber, N.I. Stilianakis, J. Infect. 57 (2008) 361–373.
[63] A.V. Berenov, J.L. MacManus-Driscoll, J.A. Kilner, Solid State Ion. 122 (1999) 41–49.
[64] F. Bridges, C.H. Booth, M. Anderson, et al., Phys. Rev. B 63 (2001) 214405.
[65] G. Dezanneau, A. Sin, H. Roussel, et al., Solid State Commun. 121 (2002) 133–137.
[66] E.L. Levytskyi, Y. Gubskyi Iu, Ukr. Biokhimicheskii Zhurnal 66 (1994) 18–30.
[67] M. Dizdaroglu, P. Jaruga, Free Radic. Res. 46 (2012) 382–419.
[68] S.J. Storr, C.M. Woolston, Y. Zhang, et al., Antioxid. Redox Signal. 18 (2013) 2399–2408.
[69] P. Moore, Vet. Rec. 175 (2014) 410.
[70] F.M. Burkle, C.M. Burkle, Disaster Med. Public Health Prep. 1 (2015) 38–43.
[71] G. Guerrier, Science 346 (2014) 434.
[72] L.A. Reperant, L.H. van de Burgwal, E. Claassen, et al., Science 346 (2014) 433–434.
[73] G.K. Donovan, Philos. Eth. Humanit. Med. 9 (2014) 15.
[74] C.S. Brown, I.M. Cropley, Postgrad. Med. J. 90 (2014) 610–612.
[75] L.H. Elliott, M.P. Kiley, J.B. McCormick, Virology 147 (1985) 169–176.
[76] H. Feldmann, H.D. Klenk, A. Sanchez, Arch. Virol. Suppl. 7 (1993) 81–100.
[77] E.O. Freed, J. Virol. 76 (2002) 4679–4687.
[78] J.M. Licata, M. Simpson-Holley, N.T. Wright, et al., J. Virol. 77 (2003) 1812–1819.
[79] J. Timmins, G. Schoehn, S. Ricard-Blum, et al., J. Mol. Biol. 326 (2003) 493–502.
[80] T. Irie, J.M. Licata, R.N. Harty, Virology 336 (2005) 291–298.
[81] A. Palencia, J.C. Martinez, P.L. Mateo, et al., Acta Crystallogr. D Biol. Crystallogr. 62 (2006) 458–464.
[82] S. Yamayoshi, Y. Kawaoka, J. Infect. Dis. 196 (Suppl. 2) (2007) S291–S295.
[83] S. Urata, T. Noda, Y. Kawaoka, et al., J. Virol. 81 (2007) 4895–4899.
[84] M. Zhadina, P.D. Bieniasz, PLoS Pathog. 6 (2010) e1001153.
[85] Y. Liu, M.S. Lee, M.A. Olson, et al., Adv. Virol. (2011) (2011) 341816.
[86] J. Lu, Z. Han, Y. Liu, et al., J. Virol. 88 (2014) 4736–4743.
[87] J. Martin-Serrano, T. Zang, P.D. Bieniasz, Nat. Med. 7 (2001) 1313–1319.
[88] T. Noda, S. Watanabe, H. Sagara, et al., J. Virol. 81 (2007) 3554–3562.